

# Data-Driven Digital Twins for Power Estimations of a Solar Photovoltaic Plant

Michael Walters, *IEEE Student Member*  
Realtime Power and Intelligent Systems  
Laboratory  
*Holcombe Department of Electrical and  
Computer Engineering*  
Clemson University, Clemson, United States  
[mawalters@ieee.org](mailto:mawalters@ieee.org)

John Yonce, *IEEE Student Member*  
Realtime Power and Intelligent Systems  
Laboratory  
*Holcombe Department of Electrical and  
Computer Engineering*  
Clemson University, Clemson, United States  
[johnyonce@ieee.org](mailto:johnyonce@ieee.org)

Ganesh K. Venayagamoorthy, *IEEE Fellow*  
Realtime Power and Intelligent Systems  
Laboratory  
*Holcombe Department of Electrical and  
Computer Engineering*  
Clemson University, Clemson, United States  
[gkumar@ieee.org](mailto:gkumar@ieee.org)

**Abstract**—Renewable energy generation sources (RESS) are gaining increased popularity due to global efforts to reduce carbon emissions and mitigate effects of climate change. Planning and managing increasing levels of RESSs, specifically solar photovoltaic (PV) generation sources is becoming increasingly challenging. Estimations of solar PV power generations provide situational awareness in distribution system operations. A digital twin (DT) can replicate PV plant behaviors and characteristics in a virtual platform, providing realistic solar PV estimations. Furthermore, neural networks, a popular paradigm of artificial intelligence may be used to adequately learn and replicate the relationship between input and output variables for data-driven DTs (DD-DTs). In this paper, DD-DTs are developed for Clemson University's 1 MW solar PV plant located in South Carolina, USA to perform realistic solar PV power estimations. The DD-DTs are implemented utilizing multilayer perceptron (MLP) and Elman neural networks. Typical practical results for two DD-DT architectures are presented and validated.

**Keywords**—Digital twin, neural network, power estimation, solar photovoltaic

## I. INTRODUCTION

The electric power generation industry is evolving because of the ever-rising energy demand, global decarbonization legislation, and heightened awareness of the negative effects of climate change. Therefore, utility companies are prioritizing the development and inclusion of clean renewable energy sources (RESS) in their generation technology portfolios. Solar photovoltaic (PV) power plants are at the forefront of RES technology due to their scalability and distributed energy resource (DER) capability. To elaborate, solar PV plants may be utilized in rooftop settings supporting localized residential loads, campus and community microgrids and industrial farm arrays for clean energy generation. In any of these configurations, solar PV plants are subject to challenges that arise in planning and management of these systems. In this context, PV power estimations may be used to improve situational awareness in distribution control centers by providing insights to the dynamic behaviors of PV plants that arise from variable weather conditions. The estimations are computed using meteorological data and mathematical equations or advanced computational methods. Solar PV power estimations can be utilized in a variety of control center applications including expected output comparisons, everyday

system health and degradation monitoring, maintenance scheduling, aiding in return on investment (ROI) calculations, and future site planning [1].

The concept of 'twins' was initially introduced in product life cycle testing during NASA's Apollo space program [2]. Digital twins (DTs) were first introduced in the manufacturing industry, making a profound impact by enabling the virtual representation factories, resources and workforces [2]. Today, DTs are gaining progressive popularity in both academia and industry settings across multiple disciplines including manufacturing, healthcare, aerospace engineering and electrical engineering. Within power systems, DTs have been developed for applications in utilities, distributed energy management systems, operation centers, fault diagnostics and renewable energy generators [3]. In each of these disciplines and/or applications, DTs have proven to be powerful tools due to their ability to represent a physical reality within a virtual environment. Data-driven DTs (DD-DTs) are developed and implemented based on measured data, providing a reliable virtual reproduction of attributes and behaviors of entities in the physical world [4]. PV plant DD-DTs offer a platform to virtually represent the plant and estimate its power generation. Therefore, a reliable, adaptable and up-to-date virtual representation of PV plants can be created using DTs to further improve understanding of their complex nature and operational dynamics in distribution power systems.

In this paper, the development and implementation of data-driven digital twins for solar PV power estimations of a 1 MW solar PV plant located at Clemson University, South Carolina, USA is studied. Two types of neural networks are used to learn the relationship between input and output variables from measured data, without explicit knowledge of the system. Internet of things (IoT) devices provide environmental data needed to construct a historical dataset and supply real-time data to the DD-DT. Typical results for multilayer perceptron and Elman neural networks are presented.

The remaining sections of the paper are as follows: Section II introduces DTs for solar PV power estimations. Section III describes the implementation of DTs. Typical DT results, discussions and their applications are presented in Section IV. Finally, Section V provides the conclusion and some directions for future work.

This research is funded by US NSF grant CNS 2131070, ECCS 2234032, CNS 2318612 and the Duke Energy Distinguished Professor Endowment Fund. Any opinions, findings and conclusions or recommendations expressed in this material are those of author(s) and do not necessarily reflect the views of NSF and Duke Energy.

Authorized licensed use limited to: University of Pretoria. Downloaded on September 30, 2024 at 21:17:47 UTC from IEEE Xplore. Restrictions apply.

## II. DIGITAL TWINS FOR SOLAR PV POWER ESTIMATION

Research and deployment of digital twins are drawing attention of the respective communities due to their capabilities to contribute to efficient operation and management of complex systems. DTs are characterized in [4] as consisting of a physical reality, virtual representation, and interconnection between them. Physical realities can be decomposed into the following parts: physical system, physical environment and physical process. A physical system consists of interacting entities, ranging from subcomponents of a single piece of machinery to all interconnected systems of a single asset. A physical environment refers to the surroundings of which the physical system resides and interacts with. Generally, this information is sourced with a variety of environmental sensors. Physical processes are how the physical system itself interacts with its physical environment. In the same manner of the physical reality, a virtual representation must include a virtual system, environment and process. A virtual system contains data and models derived from the physical system. As the name suggests, a virtual environment is simply a virtual representation of the physical environment. Virtual processes contain computational models that accurately characterize a physical process. Finally, the data and information are exchanged utilizing the interconnection component.

Data-driven digital twins (DD-DTs) are built using both historical data and real-time data as opposed to using a physics-based model. DD-DTs provide an up-to-date, reliable virtual representation of a physical reality, without explicit knowledge of specific physical components [5]. This allows data-driven approaches for estimation DTs to be highly adaptable and scalable. Through the use of IoT devices, a greater perspective of the physical environment may be obtained, further improving properties of DD-DTs. The higher the density of these devices, the more comprehensive the data will be when building the DD-DT. Approaches using artificial intelligence (AI) become even more adaptable and scalable due to fast learning. AI is able to use data captured by IoT sensors to learn the relationships between inputs and outputs in the system. The characteristics of RESs vary across different locations but can be learned and replicated by DD-DTs integrated for these sites.

As DERs continue to increase in volume, their operations increase in complexity. RESs such as PV plants wind plants are dynamic systems and have variable power output associated with weather conditions. Solar PV plants have different characteristics and may be similar to others, but no two sites are the same [6]. DTs can be implemented at PV sites to gain some insights to the nonlinear properties, relationships and reactions in their physical reality. More specifically, a virtual representation of these systems may provide increased understanding of their components based on the present level of abstraction. Furthermore, the progressive penetration of IoT devices into power systems simpler methods for DD-DTs to be implemented for PV plants with little change to the existing infrastructure. This is because IoTs provide an efficient approach to data collection, providing real-time environmental data for developing a virtual environment. Utilizing AI within the DTs enables accurate representation of the physical process. An increased understanding of these qualities introduces a source of reliable information, leading to more efficient

integration, operation, and management of PV plants, in an otherwise volatile setting.

Fig. 1 shows a representation of the implemented DD-DT for Clemson University's R-06 1MW solar PV plant. In Fig. 1, the three components characterizing DTs are shown. First, the physical reality is shown in the upper portion. Here, the physical system consists of the PV plant, weather station and micro-PMU. Meteorological conditions compose the physical environment. Information on the physical environment is captured by the IoT devices. These include solar irradiance ( $SI$ ) and temperature ( $T$ ), both measured at the weather station and PV power measured by the micro-PMU ( $P_{PV}$ ). The physical process is additionally represented here with the PV panels and corresponding power inverters. Clemson University's local area network (LAN) provides the interconnection between physical reality at the R-06 site to the DD-DTs, implemented in the Real-Time Power and Intelligent Systems (RTPIS) Laboratory. Here, the virtual representation comes to life, as the DD-DT characterizes the physical system, environment and processes.

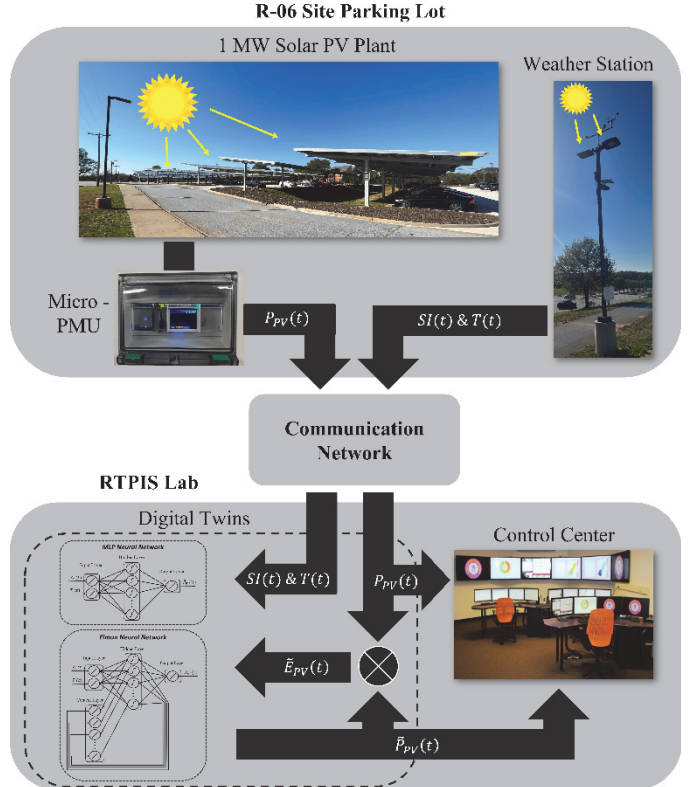


Fig. 1. Digital twin of the R-06 parking lot PV plant. The physical reality consists of 1 MW PV plant, weatherstation and micro-PMU.

## III. IMPLEMENTATION OF ESTIMATION DIGITAL TWIN

To implement a data-driven digital twin, a variety of neural networks (NNs) are utilized due to their universal approximation of nonlinear functions and behaviors capabilities. NNs have been shown to model solar PV plants with superior accuracy, as concluded in a review study in [7]. NNs do not require knowledge of specific mathematics or physics based equations to relate various parameters. NNs consist of a network of neurons and synaptic weights. The synaptic weights are updated through a training procedure until a permissible error and/or

iteration limit is reached [8]. On the other hand, traditional physics-based models require explicit knowledge of system parameters that are often unknown and static.

In the context of PV plants, a NN-based DD-DT must capture properties, characteristics and behaviors of the physical process. To elaborate, the physical process for Clemson University's 1 MW PV plant involves conversion of light energy to electrical energy by solar cells and inversion of DC to AC PV power on 17 different solar array canopies. The AC PV power is then combined at a junction point and measured by a micro-PMU, as pictured in Fig. 2. Different approaches would be subject to varying levels of abstraction when characterizing the physical system. For example, one may choose to virtually represent each component of the physical system (canopies, PV panels and inverters) separately. However, in our case, a high level of abstraction is used to characterize all 17 canopies, junction and measurement of AC PV power as the physical system. Thus, the virtual process must represent these components accordingly.

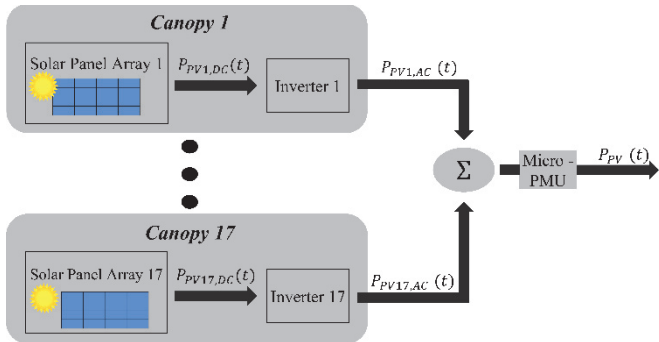


Fig. 2. Physical process at R-06 PV plant. The plant consists of 17 canopies ranging from 50kW – 60kW, each containing a solar panel array and inverter.

Specifically for this study, two neural networks are trained with meteorological data to learn the input/output relationship with generated PV power. The NNs model the solar PV plant as a whole entity, thus, in addition to learning an input/output relationship, system parameters such as partial shading and component degradation due to aging are further included in the model. A physics-based model for estimating solar PV power is proposed in (1) and represents the input/output relationship both NNs are learning

$$P_{PV}(t) = \frac{SI(t)}{SI_{ref}} P_{ref,mp} [1 + \gamma(T(t) - T_{ref})] \quad (1)$$

where  $P_{PV}$  is the estimated PV power,  $SI$  is solar irradiance,  $SI_{ref}$  is reference solar irradiance,  $P_{ref,mp}$  is the maximum PV power reference,  $\gamma$  is the solar array coefficient,  $T$  is temperature and  $T_{ref}$  is reference temperature. Note that  $SI_{ref}$ ,  $P_{ref,mp}$ ,  $\gamma$  and  $T_{ref}$  are strict parameters relating to the properties of a given solar array.

The neural network architectures implemented in this study include a multilayer perceptron (MLP) NN and an Elman NN. Both NNs utilize the same set of meteorological inputs, solar irradiance and temperature at time  $t$  to estimate PV power.

#### A. MLP Neural Network

A MLP NN features a feedforward architecture consisting of an input layer, hidden layer and output layer represented in Fig. 2. Each node represents a single neuron and accompanying transfer function, linear for input and output layers, and sigmoid for the hidden layer. The edges represent synaptic weights ( $W$  and  $V$ ) between different layers. The input weight matrix,  $W$ , connects the input layer to the hidden layer, and output weight matrix,  $V$ , connects the hidden layer with the output layer. Combining the input matrix containing solar irradiance and temperature with synaptic weight matrices forms the relationship to estimate PV power, as seen in (2) [8]. With a simpler network design, MLP NNs excel in fast paced computations due to reduced computational requirements. 15 hidden layer neurons are determined to be sufficient in capturing the nonlinear dynamics of solar PV plants, while balancing computational stress. This creates a MLP NN of size  $2 \times 15 \times 1$  with 45 synaptic weights.

$$\tilde{P}_{PV, \text{MLP}}(t) = f_{Est}(SI(t), T(t), W, V) \quad (2)$$

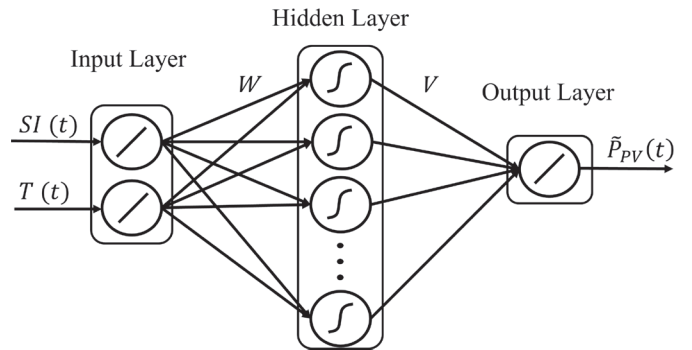


Fig. 3. MLP neural network with inputs  $SI(t)$  and  $T(t)$  as implemented to characterize the physical process shown in Fig. 2.

#### B. Elman Neural Network

An Elman NN features a recurrent architecture consisting of four layers: input, hidden, context and output which is represented in Fig. 3. The neurons, transfer functions and synaptic weights are represented in the same manner as the MLP NN. The context layer consists of the hidden layer output matrix,  $D$ , featuring linear neurons. This layer is time-delayed and fed back to the input matrix, thus memory is introduced in this architecture. This creates a relationship to estimate PV power based on solar irradiance, temperature,  $W$ ,  $V$ , at time  $t$  and  $D$  at the previous instant, seen in (3). However, as more neurons in the hidden layer are introduced, the input layer grows to incorporate these values, thus computational requirement increase. An Elman NN is implemented with six hidden layer neurons creating a NN size  $(2 + 6) \times 6 \times 1$  with 56 synaptic weights. While a smaller hidden layer can impact performance, the computational requirements during training remained approximately equivalent for MLP and Elman NNs.

$$\tilde{P}_{PV, \text{Elman}}(t) = f_{Est}(SI(t), T(t), W, V, D(t-1)) \quad (3)$$

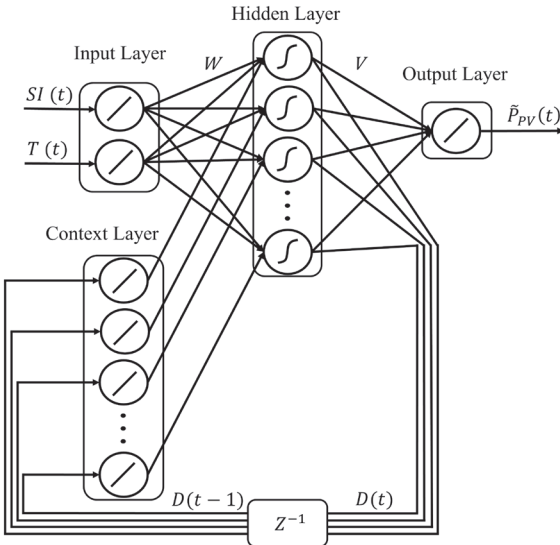


Fig. 4. Elman neural network with inputs  $SI(t)$ ,  $T(t)$  and  $D(t-1)$  as implemented to characterize the physical process shown in Fig. 2.

### C. Training Procedure

The collected dataset consists of historical solar irradiance, temperature PV power data from 86 days ranging from March 2023 to June 2023 polled every minute (approximately 360,000 data points) in Clemson, South Carolina, USA. This provides a wide variety of weather conditions, solar irradiance profiles, temperature profiles and cloud coverage. Collected data undergoes a filtering process where outlying data points resulting from faulty measurements or lost data are removed to further improve correlation. Next, variables are normalized to the range  $[0, 1]$  based on standard deviation and statistical mean.

Due to the nature of PV power estimation DTs, a progressive time dependency is not present in the data. Rather, solar irradiance and temperature are presented at a specific time  $t$ , and the corresponding PV power estimate for the same instance is calculated. Therefore, a batch training algorithm is utilized for network training. Batch calculations feature large matrices containing input data, intermediate variables and weights, further improving computational speed while training. To begin training, the synaptic weights are initialized to random values. The backpropagation algorithm discussed in [8] is utilized to update weights for the NN. This is done over a set number of iterations where error values between measured and estimated PV power are calculated. To further improve computational efficiency, an attention-based training approach is implemented to fine-tune synaptic weights. This is done by identifying intervals of high error and amplifying the calculated error signal, increasing the impact during training.

## IV. RESULTS, DISCUSSIONS & APPLICATIONS

This section presents DT implementation results and discussion in Section IV. A and potential applications in Section IV. B.

### A. Results & Discussion

Both neural networks are trained until a 1000 iteration limit is achieved. Fig. 5 displays the average MSE progression across 100 trials of back propagation training.

After training is completed, the DTs are tested over 21 days under highly variable weather conditions. To better understand and compare performances of the DTs, the 21-day dataset is classified based on cloud coverage and solar irradiance variations. This provides the opportunity to further tune NN parameters to account for high volatility in weather data. Sample results for both NNs based on weather classification are shown as follows: Figs. 6, 7, 8 and 9 for a clear day, partially cloudy day, moderately cloudy day, and mostly cloudy day, respectively.

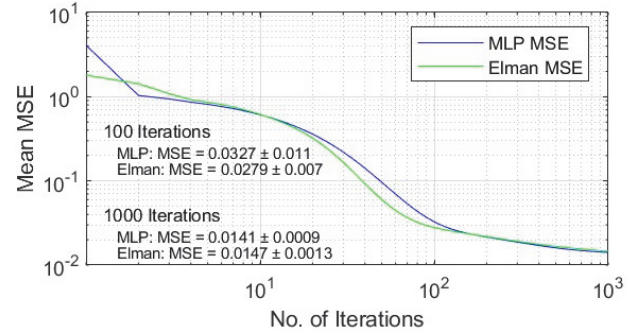


Fig. 5. MSE progression shown for MLP (blue) and Elman (green) NNs with training for 1000 iterations.

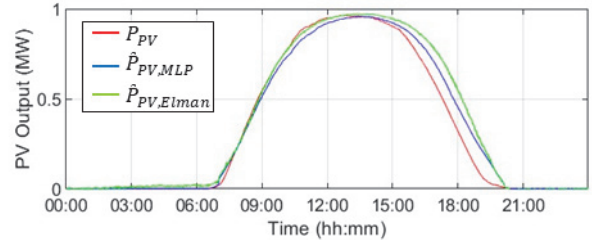


Fig. 6. Sample clear day with measured PV power (red) MLP NN estimated PV power (blue) and Elman NN estimated PV power(green).

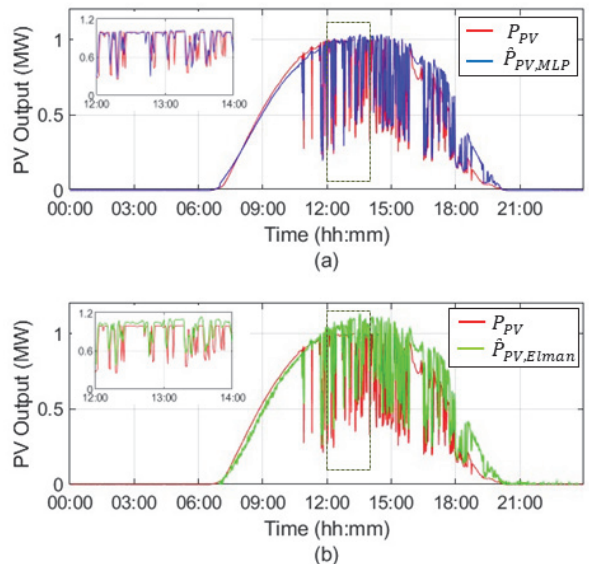


Fig. 7. Sample partially cloudy day comparing measured PV power (red) with (a) MLP NN estimated PV power and (b) Elman NN estimated PV power.

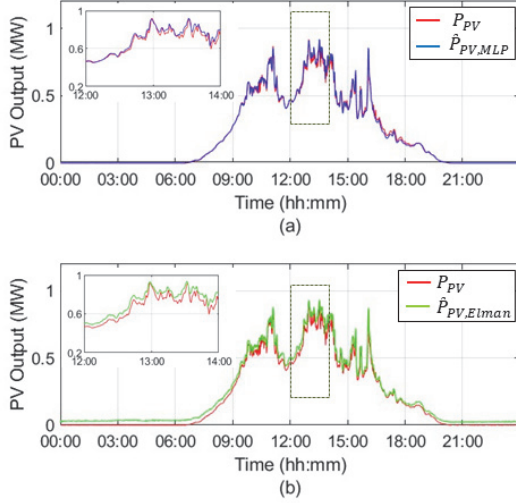


Fig. 8. Sample moderately cloudy day comparing measured PV power (red) with (a) MLP NN estimated PV power and (b) Elman NN estimated PV power.

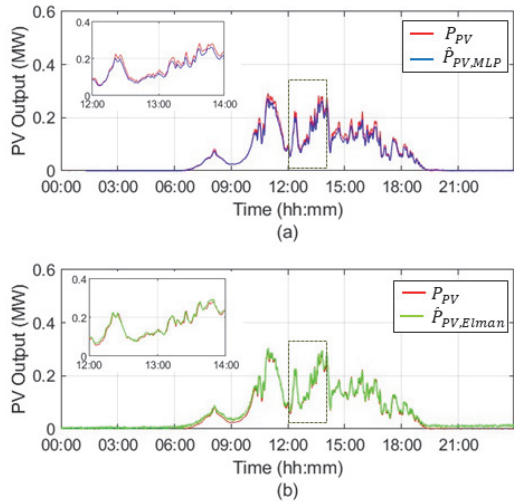


Fig. 9. Sample mostly cloudy day comparing measured PV power (red) with (a) MLP NN estimated PV power and (b) Elman NN estimated PV power.

Training performance displayed in Fig. 5 reveals some characteristics of MLP and Elman NNs. Averaging MSE training for both networks over 1000 iterations results in nearly the same training MSE, 0.0141 for MLP and 0.0147 for Elman with standard deviations on the order of  $10^{-3}$ . However, at 100 iterations, MSE for MLP is 0.0327 and 0.0279 for Elman, with standard deviations on the order of  $10^{-2}$ . Evidently, through

first portion of training, the Elman NN had significantly lower MSE, signifying a faster learning rate, but both architectures tended to converge to similar MSE values at 1000 iterations. This trend may be contributed to similar network sizes between architectures (45 weights for MLP and 56 weights for Elman).

As seen in Figs. 6 - 9 both DTs are capable of estimating PV power with some variations in performances between both DTs. The clear day sampled in Fig. 6 proved to be a difficult day for the DTs to estimate. While the profile of the measured PV power curve is preserved, peak and falling edge information is skewed. A sampled partially cloudy day is featured in Fig. 7. Similarly, to the clear day, estimates captured the general profile of measured PV power, but still struggled to capture variation, peak and falling edge information. Shortcomings for these two weather conditions may be explained by a lower correlation between input weather data and measured PV power. For the moderately cloudy and mostly cloudy samples pictured in Figs. 8 and 9, respectively, the performances of both models are very accurate. Rising edge, peak and falling edge information are accurately captured for these weather conditions. This trend may be contributed to a higher correlation between solar irradiance and measured PV power for these days.

Table I summarizes performance metrics for both MLP and Elman NNs in comparison to a statistical approach utilizing an ARIMA model [9]. Calculations for mean absolute percent error (MAPE) and mean square error are given for each weather classification based on daytime and nighttime intervals. Comparing both NNs, the Elman NN is slightly more accurate with daytime clear and partially cloudy weather conditions. On the other hand, MLP NN estimations are more accurate with daytime moderately cloudy, mostly cloudy and nighttime conditions for every classification. These trends may be explained by the hidden layer size for each architecture. A greater number of neurons increases computational power and performance when approximating nonlinear relationships. Increasing the number of neurons in either architecture could perhaps improve performance at the expense of computational burden. Comparing the MAPEs of both NNs to the ARIMA model reveals greater estimation accuracy with the NNs for moderately and mostly cloudy conditions. This can be attributed to the highly variable power generation of solar PV plants on days with these classifications. However, the ARIMA model outperformed both NNs in clear daytime and nighttime conditions and in partially cloudy nighttime conditions. Overall, the NNs outperform the ARIMA model during daytime conditions with cloud cover.

The coefficients of determination ( $R^2$ ) shown in Figs. 10 and 11 shows the accuracy of PV power estimations compared to the actual measurement. An ideal 1:1 line is additionally plotted to

TABLE I. DIGITAL TWIN PERFORMANCE COMPARISON

Weather Profile	MLP Neural Network			Elman Neural Network			Daytime MAPE (%)	Daytime MSE	Nighttime MSE
	Daytime MAPE (%)	Daytime MSE	Nighttime MSE	Daytime MAPE (%)	Daytime MSE	Nighttime MSE			
Clear	28.15	$4.84 \times 10^{-3}$	$5.91 \times 10^{-6}$	26.11	$4.33 \times 10^{-3}$	$1.88 \times 10^{-4}$	<b>5.12</b>	$1.68 \times 10^{-4}$	$3.99 \times 10^{-7}$
Partly Cloudy	31.22	$2.11 \times 10^{-2}$	$5.81 \times 10^{-7}$	29.52	<b><math>2.09 \times 10^{-2}</math></b>	$2.03 \times 10^{-4}$	<b>22.2</b>	$2.50 \times 10^{-2}$	<b><math>5.41 \times 10^{-7}</math></b>
Moderately Cloudy	<b>1.93</b>	<b><math>4.87 \times 10^{-4}</math></b>	<b><math>2.93 \times 10^{-7}</math></b>	7.45	$1.14 \times 10^{-3}$	$8.18 \times 10^{-4}$	8.21	$1.40 \times 10^{-3}$	$4.04 \times 10^{-7}$
Mostly Cloudy	<b>5.22</b>	<b><math>6.70 \times 10^{-5}</math></b>	<b><math>3.72 \times 10^{-7}</math></b>	6.41	$7.77 \times 10^{-4}$	$1.91 \times 10^{-4}$	13.00	$3.13 \times 10^{-4}$	$7.67 \times 10^{-7}$

show ideal correlation. The coefficient of determination is calculated using (4),

$$R^2 = 1 - \frac{\sum(P_{PV, i} - \bar{P}_{PV})^2}{\sum(P_{PV, i} - \bar{P}_{PV})^2} \quad (4)$$

where  $P_{PV, i}$  is the  $i$ th measured power,  $\bar{P}_{PV, i}$  is the  $i$ th estimated power and  $\bar{P}_{PV}$  is the mean measured power. In both cases, MLP and Elman NNs accounted for over 97% of variation.

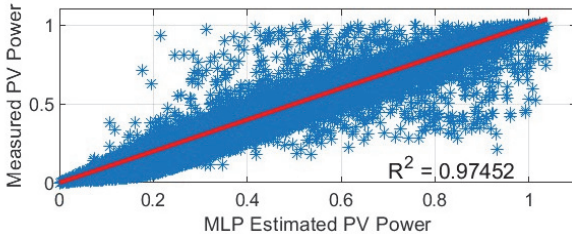


Fig. 10. MLP estimated PV power vs. measured PV power.

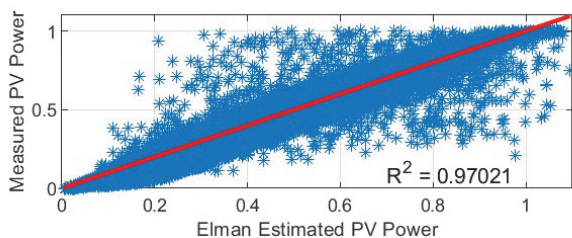


Fig. 11. Elman estimated PV power vs. measured PV power.

### B. Applications of Estimation Digital Twin

Estimation-based DTs offer a variety of applications for solar PV site planning and enhanced situational awareness in distribution center operation and management. Comparison of measured and estimated PV power enable PV plant performance monitoring by alerting operators when sustained discrepancies occur. In these instances, PV panels may require cleaning or repair. In addition to providing these alerts, DTs may be able to identify the affected panels [10]. Over time, progressive learning updates will allow the DT to account for PV plant performance degradation. System aging may be tracked by periodically recording and comparing DT estimations [11]. Finally, estimation-based DTs can provide intelligence when planning future PV plant sites of any size due to their scalability and adaptability. This includes reliable PV power output expectations and return-on-investment planning for PV plants ranging from rooftop setups to distributed generation [12].

### V. CONCLUSION

In the electric power generation industry with increasing levels of distributed renewable energy sources, reliable and trustworthy sources of information providing situational awareness are necessary in distribution operational control centers. In addition to an increased understanding of nonlinear PV plant behaviors, data-driven digital twins (DD-DTs) provide information for planning and managing PV plant sites in distributed networks. In this study, DD-DTs for Clemson University's 1 MW PV plant were developed with PV power

estimations. These DD-DTs have shown the capability of capturing PV plants behaviors and characteristics using static and dynamic neural networks. Categorizing days based on meteorological conditions enabled the comparison of performances of DD-DTs.

In future work, implementing a higher density network of distributed IoT devices will lead to greater accuracy and modularity of DD-DTs. Obtaining data from individual modules in the physical process will provide detailed abstraction when characterizing the physical system of Clemson University's R-06 PV plant. Further tuning of neural network parameters will maximize accuracy while minimizing computational expense. Lastly, new applications can be explored in order to more fully utilize capabilities of DD-DTs.

### ACKNOWLEDGMENT

The authors acknowledge the facilities provided by the Real-Time Power and Intelligent Systems (RTPIS) Laboratory and physical facilities at Clemson University, SC, USA for the research carried out for this paper.

### REFERENCES

- [1] D. M. Riley and G. K. Venayagamoorthy, "Characterization and modeling of a grid-connected photovoltaic system using a Recurrent Neural Network," in Proc. *The 2011 International Joint Conference on Neural Networks*, pp. 1761-1766
- [2] M. Liu, S. Fang, H. Dong, and C. Xu, "Review of digital twin about concepts, technologies and industrial applications." *Journal of Manufacturing Systems*, vol. 58, pp. 346-361, Jan. 2021.
- [3] S. Nguyen, M. Abdelhakim and R. Kerestes, "Survey paper of digital twins and their integration into electric power systems," in Proc. *2021 IEEE Power & Energy Society General Meeting Conf.*, pp 01-05.
- [4] E. VanDerHorn, and S. Mahadevan, "Digital Twin: Generalization, characterization and implementation," *Decision Support Systems*, vol. 145, Jun. 2021.
- [5] A. Sleiti, J. Kapat, and L. Vesely, "Digital twin in energy industry: Proposed robust digital twin for power plant and other complex capital-intensive large engineering systems," *Energy Reports*, vol. 8, pp. 3704-3726, Nov. 2022.
- [6] N. Sehrawat, S. Vashisht, and A. Singh, "Solar irradiance forecasting models using machine learning techniques and digital twin: A case study with comparison." *International Journal of Intelligent Networks*, vol. 4, pp. 90-102, May, 2023.
- [7] K. Garud, S. Jayaraj, and M. Lee, "A review on modeling of solar photovoltaic systems using artificial neural networks, fuzzy logic, genetic algorithm and hybrid models," *International Journal of Energy Research*, vol.45, pp. 6-35, Jun. 2021.
- [8] V. G. Gudise, and G. K. Venayagamoorthy, "Comparison of particle swarm optimization and backpropagation as training algorithms for neural networks," in Proc. *2003 IEEE Swarm Intelligence Symposium Conf.*, pp. 110-117.
- [9] H. Sharadga, S. Hajimirza, and R. S. Balog, "Time series forecasting of solar power generation for large-scale photovoltaic plants," *Renewable Energy*, vol. 150, pp. 797-807, May 2020.
- [10] M. Toothman, B. Braun, S. Bury, M. Dessauer, K. Henderson, S. Phillips, Y. Ye, D. Tilbury, J. Moyne, and K. Barton, "A digital twin framework for mechanical system health state estimation," *IFAC-PapersOnLine*, vol. 54, pp. 1-7, 2021.
- [11] A. Mellit, and S. Kalogirou, "Artificial intelligence and internet of things to improve efficacy diagnosis and remote sensing of solar photovoltaic systems: Challenges, recommendations and future directions," *Renewable and Sustainable Energy Reviews*, vol. 143, Jun. 2021.
- [12] L. Naing, and D. Srinivasan, "Estimation of solar power generating capacity," in Proc. *2010 IEEE International Conference on Probabilistic Methods Applied to Power Systems Conf.*, pp. 95-101.